MIPAS-ENVISAT limb-sounding measurements: trade-off study for improvement of horizontal resolution

Marco Ridolfi, Luca Magnani, Massimo Carlotti, and Bianca Maria Dinelli

The Michelson Interferometer for Passive Atmospheric Sounding (MIPAS) is a limb-scanning spectrometer that has operated onboard the Environmental Satellite since the end of March 2002. Common features of limb-scanning experiments are both high vertical resolution and poor horizontal resolution. We exploit the two-dimensional geo-fit retrieval approach [Appl. Opt. **40,** 1872–1875 (2001)] to investigate the possibility of improving the horizontal resolution of MIPAS measurements. Two different strategies are considered for this purpose, one exploiting the possibility (offered by the geo-fit analysis method) for an arbitrary definition of the retrieval grid, the other based on the possibility of saving measurement time by degrading the spectral resolution of the interferometer. The performances of the two strategies are compared in terms of the trade-off between the attained horizontal resolution and the retrieval precision. We find that for ozone it is possible to improve by a factor of 2 the horizontal resolution, which in the nominal measurement plan is ~530 km. This improvement corresponds to a degradation of the retrieval precision, which on average varies from a factor of 1.4 to 2.5, depending on the adopted spectral resolution.

OCIS codes: 010.1280, 010.1290, 010.4950, 280.0280, 280.1120, 070.4790.

1. Introduction

The Michelson Interferometer for Passive Atmospheric Sounding (MIPAS) is an Earth-observation instrument, developed by the European Space Agency (ESA), operating onboard the Environmental Satellite (ENVISAT) that was successfully launched on a nearly polar orbit on 1 March 2002. The instrument is based on a high-resolution Fourier-transform spectrometer and is designed to provide continuous information on a number of atmospheric species that are relevant to several interlinked problems over ozone chemistry and global change. MIPAS measures the emission of the atmosphere in a wide spectral interval in the mid-IR with the limb-scanning observation technique. For ~80% of the measuring time, MIPAS is planned to operate in its nominal observation mode, which consists of measuring consecutive backward-looking limb-scans with the lines of sight lying approximately in the orbit plane. Each limb-scan consists of 17 observation geometries with tangent altitudes ranging from 6 to 68 km with steps of 3 or 5 km. In the nominal mode the spectral resolution of the instrument is set to its maximum value of 0.035 cm^{-1} full width at half-maximum, unapodized, achieved with a maximum optical path difference of 20 cm.

MIPAS spectra are analyzed by the ESA's ground processor that provides in near-real time (NRT) (less than 3 h from data acquisition) pressure at the tangent points, the vertical distribution of temperature, and the volume mixing ratio of six key species (H_2O, O_3, HNO_3, CH_4, N_2O, and NO_2).

For the analysis of the measurements, ESA's ground processor uses a retrieval algorithm[1] based on the global-fit[2] approach. In this algorithm the portion of the atmosphere sounded by the line of sight of the instrument is assumed to be horizontally homogeneous, and observations of a full limb-scan are simultaneously processed to infer a vertical distribution profile. Therefore a one-to-one correspondence exists between the measured limb-scans and the retrieved profiles. The latter are naturally associated with a geographical coordinate, here, according to ESA convention, calculated as the arithmetic mean of the geographical coordinates of the tangent points of the corresponding limb-scan. The spatial resolution of the geophysical parameters re-

M. Ridolfi and M. Carlotti are with the Dipartimento di Chimica Fisica e Inorganica, Università di Bologna, Viale del Risorgimento 4, 40136, Bologna, Italy (e-mail for M. Ridolfi, ridolfi@fci.unibo.it). L. Magnani and B. M. Dinelli are with the Istituto di Scienze dell' Atmosfera e del Clima, Consiglio Nazionale delle Ricerche, Via Gobetti 101, 40129, Bologna, Italy.

Received 25 September 2003; revised manuscript received 27 February 2004; accepted 2 July 2004.

0003-6935/04/315814-11$15.00/0

trieved by the global-fit (unconstrained) approach is determined as follows:

(a) In the altitude domain: by the vertical sampling step of the instrument, the instrument field of view (FOV) (~4 km vertically), and the chosen retrieval grid.
(b) In the horizontal domain: by the horizontal separation between subsequent limb-scans (~530 km at the Earth's surface in the nominal observation mode).

In general the spatial resolution (both vertical and horizontal) and the random error (precision) of the retrieval are linked to each other. Curves showing the trade-off of the random error as a function of the vertical resolution were first proposed by Backus and Gilbert[3] in 1970. Details of the calculation of trade-off curves were illustrated for practical remote sensors by Conrath[4] in 1972. More recently several authors[5–7] have studied the trade-off between the vertical resolution and the precision of the retrieval in the case of limb-sounding measurements. For the MIPAS instrument, theoretical studies[8] have shown that, in the frame of unconstrained analyses, it is not worthwhile to perform the retrievals on a vertical grid finer than the vertical sampling step of the MIPAS observations. Actually, if no regularization[9] is used, a vertical spacing between the retrieved data points finer than the measurement vertical grid leads to large oscillations in the retrieved profiles. Because of these considerations, ESA's NRT processor retrieves the target quantities at altitudes identified by the tangent points of the measurements, whereas the horizontal resolution is determined by the separation between subsequent scans. However, so far, there have been no theoretical studies demonstrating that MIPAS observations do not contain enough information to retrieve profiles with horizontal separations smaller than the actual separation between the measured scans.

Recently, a new two-dimensional retrieval approach named geo-fit, introduced by Carlotti *et al.*,[10] opened the possibility of also studying the trade-off between horizontal resolution and precision for along-track satellite limb-sounding measurements. The geo-fit approach is based on the simultaneous inversion of all the limb-scans measured along an entire orbit. This approach is applicable to measurements operated along the orbit track and makes it possible to model the horizontal variability of the atmosphere. In the geo-fit the retrieval grid is fully independent from the measurement grid; therefore it is realistic to consider the possibility of retrieving atmospheric profiles with horizontal separations smaller than those of the measured scans at the cost of degraded precision.

Another approach assessed here to improve the horizontal resolution relies on the technical design of the MIPAS instrument. In fact the interferometer can be operated at a reduced spectral resolution so that the acquisition time of the individual interferograms decreases, and the atmosphere can then be sampled with an increased number of limb-scans per orbit. The finer horizontal sampling enhances the horizontal resolution of the measurements. However, this strategy too is expected to have an effect on the precision of the retrieved profiles.[11]

In this paper we study the trade-off between the horizontal resolution and the precision of the retrieved profiles, exploiting the capabilities of the geo-fit approach applied to MIPAS observations. To modify the horizontal resolution, we consider separately the two possible approaches outlined above.

(a) The definition of the retrieval grid in the inversion of full-spectral-resolution measurements.
(b) The degradation of the spectral resolution and retrieval of one vertical profile per measured limb-scan.

The trade-off study reported in this paper is based on the retrieval of ozone, a species that, especially in hole conditions, would greatly benefit by an improved horizontal resolution.

The quantitative findings reported in this paper are applicable only to the MIPAS experiment. However, the method can be extended to any satellite limb-scanning instrument measuring the atmosphere along the orbit track.

The test retrievals carried out in this study have been performed on synthetic observations. This strategy allows for proof, for each retrieval setup, of the consistency of our forward and retrieval schemes by means of comparing the retrieved profiles with the true atmospheric profiles adopted for the generation of the synthetic observations.

In Section 2 we recall the basic formalism of the geo-fit retrieval approach. In Section 3 we explain how the trade-off tests are set up and the criteria adopted for evaluating the retrieval performance. In Section 4 we discuss the trade-off tests performed by varying the retrieval grid, while in Section 5 we discuss the trade-off studies performed, acting on the spectral resolution. In Section 6 we compare the two strategies and draw the conclusions of the study.

2. Geo-fit Retrieval Algorithm

The geo-fit algorithm used in the studies presented in this paper has been described fully in Ref. 10. In this section we briefly recall the rationale and the basic equations of this retrieval approach.

In a limb-sounding measurement the signal that reaches the spectrometer is determined by the radiative-transfer processes that occur along the entire line of sight. In most retrieval algorithms the observations are simulated, assuming that the observed atmosphere is horizontally homogeneous; it follows that the retrieved profiles are affected by a systematic error deriving from this assumption. In the geo-fit approach the assumption of horizontal homogeneity of the atmosphere is no longer used. This means that each limb observation is exploited to determine the unknown quantity at a number of loca-

tions among those spanned by each limb observation's line of sight. Inversion analyses that attempt to derive atmospheric parameters at different locations along the line of sight usually face an ill-posed problem that prevents the successful retrieval of the desired quantity. In a satellite instrument sounding the atmosphere along the orbit track, the problem that arises when the assumption of horizontal homogeneity is no longer applied can be solved by exploiting the fact that limb-scanning measurements are continuously recorded along the orbit, and the lines of sight of a given scan sound atmospheric portions that are also sounded by the observations of nearby scans. This means that information on a given location in the atmosphere can be gathered from all the lines of sight that cross that location whatever scan they belong to. Since the loop of cross talk between nearby scans closes when the starting scan is reached again at the end of the orbit, in a retrieval analysis the entire gathering of information can be obtained by merging in a simultaneous fit the observations of an entire orbit.

The unknowns of the geo-fit retrieval are determined by using an unconstrained nonlinear least-squares fit based on the Gauss–Newton method. A theoretical description of this method, applied to the retrieval of atmospheric parameters, can be found in Refs. 1, 5, and 12. Here we recall some concepts that are used in the following sections.

The goal of the retrieval is to find an estimate $\hat{\mathbf{x}}$ of the n-dimensional vector of the unknowns (state vector) that minimizes the scalar cost function χ^2 defined as

$$\chi^2 = [\mathbf{y}_{\text{obs}} - \mathbf{y}(\hat{\mathbf{x}})]^T \mathbf{S}_y^{-1} [\mathbf{y}_{\text{obs}} - \mathbf{y}(\hat{\mathbf{x}})], \quad (1)$$

where T denotes the transpose operation, $\mathbf{y}_{\text{obs}}$ is the m-dimensional vector of the observations (containing all selected spectral radiances of all tangent altitudes of all limb-scans of the analyzed orbit), $\mathbf{y}(\hat{\mathbf{x}})$ is the m-dimensional vector of the simulations obtained from a radiative-transfer model[10] that assumes the atmospheric state $\hat{\mathbf{x}}$ [in our case, the ozone volume mixing ratio (VMR) at the selected retrieval grid points and atmospheric continuum for all spectral microwindows included in the analysis at the selected retrieval grid points], and $\mathbf{S}_y$ is the $m \times m$ covariance matrix describing the errors of the observations.

Since the dependence of $\mathbf{y}$ on $\mathbf{x}$ is typically nonlinear, the solution $\hat{\mathbf{x}}$ that minimizes the cost function [Eq. (1)] cannot be obtained by using a direct analytic expression. The Gauss–Newton method provides an iterative solution to this problem. Given an estimate $\hat{\mathbf{x}}_i$ of the state vector $\mathbf{x}$ at the ith iteration, the Gauss–Newton method provides an improved estimate $\hat{\mathbf{x}}_{i+1}$ of $\mathbf{x}$ at the iteration $i + 1$ as

$$\hat{\mathbf{x}}_{i+1} = \hat{\mathbf{x}}_i + (\mathbf{K}_i^T \mathbf{S}_y^{-1} \mathbf{K}_i)^{-1} \mathbf{K}_i^T \mathbf{S}_y^{-1} [\mathbf{y}_{\text{obs}} - \mathbf{y}(\hat{\mathbf{x}}_i)], \quad (2)$$

where $\mathbf{K}_i$ is the $m \times n$ Jacobian matrix containing the partial derivatives of the simulations with respect to the elements of the state vector at iteration i:

$$\mathbf{K}_i(j, h) = \left. \frac{\partial \mathbf{y}_j}{\partial \mathbf{x}_h} \right|_{x=\hat{x}_i}, \quad (3)$$

with $j = 1, \ldots, m$ and $h = 1, \ldots, n$. The retrieval iterations are stopped when a predefined convergence criterion is fulfilled. The solution of the retrieval is characterized by the $n \times n$ dimensional covariance matrix $\mathbf{S}_x$ given by[12]

$$\mathbf{S}_x = (\mathbf{K}^T \mathbf{S}_y^{-1} \mathbf{K})^{-1}, \quad (4)$$

where $\mathbf{K}$ is the Jacobian of Eq. (3) evaluated at convergence. The square roots of the diagonal elements of $\mathbf{S}_x$ represent the estimated standard deviations (ESDs) (or σ) of the individual retrieved parameters, i.e.,

$$\sigma_h = [(\mathbf{S}_x)_{h,h}]^{1/2} \qquad \text{with } h = 1, \ldots, n. \quad (5)$$

3. Setup of Trade-off Studies

As pointed out in Section 1, our trade-off studies consist of evaluating the retrieval precision corresponding to different retrieval setups. A significant number of test retrievals were carried out, and for each test the following steps were performed:

(1) Generation of synthetic MIPAS observations for the full orbit; calculation of the covariance matrix $\mathbf{S}_y$ of the synthetic observations.
(2) Setup of the retrieval state vector.
(3) Running of the retrieval analysis.
(4) Evaluation of the precision and the overall consistency of the retrieval setup.

At the completion of the entire set of tests, the performances of the retrievals were critically compared. In Subsections 3.A–3.C we report some details of steps (1), (2), and (4) that characterize the individual test retrievals.

A. Generation of Synthetic Observations and Their Covariance Matrix

The synthetic observations used in all the tests carried out in the frame of this study have been generated by applying an instrument model to the high-resolution limb-emission radiances simulated by a forward model. Some common features of the synthetic observations are summarized below.

1. Selection of Spectral Intervals

In analogy with ESA's NRT processor the retrieval of atmospheric profiles is performed by analyzing only a few ($\leq$10) narrow ($\leq$3 cm^{-1}) spectral intervals (called microwindows) containing relevant information on the target quantity. The microwindows used in the test retrievals of this study were selected according to an optimized procedure[13] that aimed at minimization of the total retrieval error at the retrieval altitudes.

2. Reference Atmospheric Model

The state (pressure, temperature, and composition) of the atmosphere assumed for simulation of the limb-emission radiances was calculated by using the Slimcat three-dimensional chemical transport model developed by Chipperfield.[14] This model provides pressure, temperature, and VMR altitude profiles on a grid of 7.5° in longitude and 5° in latitude except for the polar regions where the latitudinal grid is 4.5°. The state of the atmosphere was calculated on 27 September 1996 when ozone-hole conditions occurred in the Antarctic region. The atmospheric-continuum profiles were calculated by using the model described in Ref. 15.

3. Forward Model

The forward model used to generate the limb-emission radiances is described in Ref. 10. This model allows for the horizontal variability of the atmosphere sounded by the line of sight of the instrument, and, in the case of horizontal homogeneity of the atmosphere, it was validated against simulations calculated by various IR radiative-transfer models[16] available in Europe. Recently this forward model was also validated against the first available MIPAS measurements.[17]

4. Instrument Model

To allow for instrumental effects, the high-resolution limb radiances simulated by the above-mentioned forward model are convolved with the instrument line shape and the FOV response functions.[18] Afterward artificial Gaussian noise of an amplitude consistent with the instrument radiometric performance at the selected spectral resolution[18,19] is added. Finally the spectra obtained are apodized by using the Norton–Beer strong apodizing function.[20] The use of apodization is consistent with the adopted microwindow selection scheme[13] and leads to a speedup of the forward model computations. (The far lines can be disregarded if apodization is used.)

5. Satellite Orbit

For simplicity we assumed a strictly polar (and therefore closed) orbit, whereas the real ENVISAT orbit has a slight inclination of 8.5°. Recent studies[21] indicate that the assumption of closed orbit can also be applied to the analysis of real MIPAS measurements with a minor effect on the accuracy of the retrieved products. The test cases reported in this paper refer to the atmosphere sounded by MIPAS in a polar orbit that passed over Greenwich, England.

6. Covariance Matrix of the Synthetic Observations

The covariance matrix of the synthetic observations $\mathbf{S}_y$ is calculated by using the algorithm described in Ref. 19. This calculation accounts for both the noise-equivalent spectral radiance added to the spectra and the apodization process that introduces correlations among the spectral data points. In our tests, whenever the instrument spectral resolution is changed, the spectral sampling step $\Delta\sigma$ is changed according to $\Delta\sigma = 1/(2\,MPD)$ (where MPD is the actual maximum optical path difference of the measured interferogram) and no zero filling or resampling is applied.[19] The possible correlations between spectral points belonging to different microwindows are neglected.

B. Setup of the Retrieval State Vector and Retrieval Grid

The geo-fit retrieval system[10] derives the VMR distribution of the target molecular species from the observations of an entire orbit. Therefore the parameters of the retrieval are

- VMR values of the analyzed molecular species (ozone in this study) at a set of geo-located altitudes (retrieval grid),
- atmospheric continuum values at the same position of the VMR parameters for the central frequencies of the analyzed microwindows.

The spatial resolution and the precision of the retrieved profiles are generally negatively correlated[5] and strongly dependent on the grid on which the retrieved values are represented. When horizontal homogeneity is assumed, the problem of choosing the retrieval grid lies in the selection of the altitudes at which the parameters are retrieved. Since the weighting functions[5] of the observations generally peak at the tangent altitudes, a common choice is to let these altitudes coincide with the retrieval grid. In the case of a geo-fit a two-dimensional retrieval grid must be adopted, the second dimension being an angular (polar) coordinate identifying the position of the retrieval-grid points in the orbit plane. The location of the tangent points of the observations could still be the leading criterion for the choice of the retrieval grid. However, even in the case of identical elevation scans, because of the inhomogeneity of the atmosphere, the ray tracing of the observations leads to different tangent altitudes because of the different refractive indices encountered by the lines of sight. The resulting spread of the tangent altitudes would make the interpolation process difficult. Therefore in the case of two-dimensional retrievals a retrieval grid at fixed altitudes is a more suitable choice. For this reason in our tests the retrieval-grid points have been placed at the nominal altitude of the tangent points of the limb-scans, which is the altitude reached by the line of sight in the absence of refraction.

Owing to the motion of the satellite and to the finite time interval needed to acquire the limb-scans ($\approx$75 s), the tangent points of the individual views of a limb-scan are not vertically aligned (the horizontal spread being of the order of 500 km). To ease both the interpretation of the retrieval results and the interpolation process that may be required after the retrieval, we choose to have the retrieval-grid points vertically aligned rather than coinciding with the nominal tangent points of the limb measurements. In particular, if a single VMR profile is retrieved for each measured scan (which is the only feasible approach when a usual one-dimensional inversion algo-

rithm is used[1]), the retrieval grid points are vertically aligned at the average polar coordinate of the tangent points of the individual limb-scans [see Figs. 1(a) and 1(c)]. In Sections 4 and 5 the retrieval setup based on the nominal MIPAS observational mode and one retrieved profile per measured limb-scan is referred as the reference retrieval setup [Fig. 1(a)]. The initial guess of the state vector in the retrieval analysis is generated by perturbing the profiles used to simulate the observations. A random perturbation (to a maximum of $\pm 30\%$) was applied to the individual VMR profile points and a similar one (to a maximum of $\pm 50\%$) to the individual points of atmospheric continuum profiles. The applied perturbations were limited in amplitude so that the number of iterations necessary to reach the convergence is always less than three for all the retrieval setups considered in this study.

C. Criteria for Performance Evaluation

The performance of a given retrieval setup is determined by the accuracy (or total error) affecting the retrieved parameters. In the case of retrievals carried out from synthetic observations, based on a known atmospheric state, the accuracy of the retrieved profiles can be assessed through the discrepancies between retrieved and true state parameters. These discrepancies account for both the error due to measurement noise (i.e., the ESD) and the possible smoothing error[12] originating from a retrieval grid coarser than the actual spatial resolution of the adopted atmospheric model. In our case model errors (i.e., the model parameter error and the forward model error[12]) do not show up because the synthetic observations are generated by the same forward model used by the inversion algorithm. We are interested in horizontal resolutions finer than the horizontal sampling step of the nominal MIPAS measurements (4.8 deg). Therefore, to properly assess the accuracy of these retrieval setups, we need an atmospheric model with a horizontal resolution finer than the finest assessed retrieval grid (i.e., with a horizontal resolution of at least 1 deg). However, to date there are no global-coverage measurements with a spatial resolution much finer than 5 deg in latitude permitting one to globally validate atmospheric models with such a high resolution. For this reason, considering that global high-resolution atmospheric models may be unreliable,[22] we preferred to base our study on a validated atmospheric model with a relatively coarse resolution (from 4.5 to 5 deg). Although this choice prevents the assessment of smoothing errors relating to the retrieval grids of interest, it is surely suitable for assessing the trade-off between horizontal resolution and the ESD.

Since the retrieval approach used in this study is relatively new, to monitor the self-consistency of the overall forward and inverse scheme, for each retrieval setup we also evaluated the χ^2 function defined in Eq. (1) and the ${\chi_R}^2$ function (the reduced chi-square) defined as

$$ {\chi_R}^2 \equiv \frac{\chi^2}{m - n}, \tag{6} $$

where m and n are the number of analyzed spectral points and the number of retrieved parameters, respectively (see also Section 2). The expectation value of ${\chi_R}^2$ at convergence is equal to 1.[23] Values of ${\chi_R}^2$ significantly greater than one are ascribed to the following:

- The inaccurate fit of the observations due to the smoothing error possibly originating from the choice of a retrieval grid with a horizontal resolution coarser than that of the atmospheric model used to generate the synthetic observations.
- A redundant set of retrieval parameters n. If we choose a retrieval grid much finer than the horizontal structures of the atmosphere actually detected by the measurements, the retrieval parameters are not independent from one another. This means that some of the retrieval parameters do not effectively contribute to the reduction of the residuals of the fit. In this case we still have $\chi^2 \approx m$, but ${\chi_R}^2 \approx m/(m - n)$ is greater than unity because n is significant compared with m.
- Convergence error. This is the error occurring whenever the convergence criterion stops the iterative procedure before the real minimum of the χ^2 function has been reached. For all the retrieval setups in this paper the convergence criterion (a variation of χ^2 in two subsequent iterations of less than 5%) was generally fulfilled after two iterations.

As a further check of the consistency of the used forward and retrieval schemes, for each test retrieval we visually inspect the ratio between the difference retrieved − true value and the related ESD. Whenever the retrieval grid is finer than or equal to the resolution of the reference atmospheric model (i.e., whenever the smoothing errors are negligibly small), this ratio must be equal or less than unity for ~68% of the retrieved data points.[23]

4. Trade-off Study Based on the Definition of the Retrieval Grid

In this first set of trade-off tests the ozone-retrieval precision was evaluated as a function of the horizontal separation between the retrieved profiles, with the retrievals performed on synthetic observations corresponding to the MIPAS nominal observation mode.

Figure 1(a) represents (on a distorted scale) the setup with the nominal measurement grid and one retrieved profile per measured limb-scan. Figure 1(b) represents a grid in which four profiles per limb-scan of the nominal measurement grid are retrieved. The retrieved profiles are evenly distributed along the full orbit so that the horizontal separation between them identifies the horizontal resolution of the

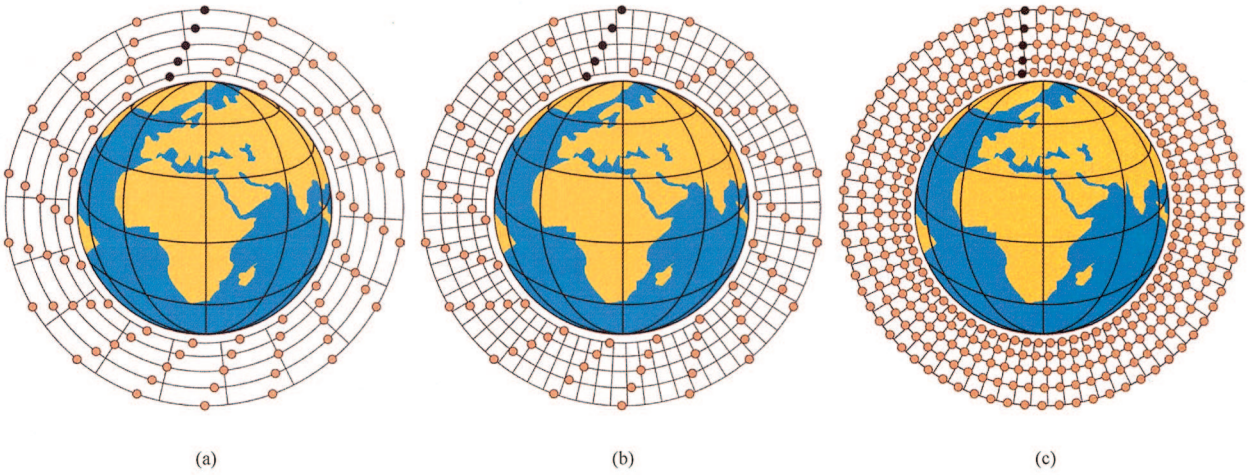

Fig. 1. Location of the tangent points of MIPAS measurements (solid circles) and possible retrieval grids (intersection between large circles and radii) (on a distorted scale): (a) nominal measurement grid, one retrieved profile per measured limb-scan; (b) nominal measurement grid, four retrieved profiles per measured limb-scan; (c) reduced spectral resolution (1/4 of nominal), one retrieved profile per measured limb-scan.

retrieved atmospheric distribution. The horizontal separation between the retrieved profiles can be expressed either in terms of the difference between the polar coordinate (degrees) of two adjacent profiles or in terms of the linear separation (kilometers) between adjacent profiles as measured at the Earth's surface. In Table 1 we summarize the horizontal resolution of the assessed retrieval grids; the boldface entries refer to the reference-retrieval grid in which one ozone profile per measured limb-scan is retrieved.

In Fig. 2 we show as a function of the horizontal resolution (identified on the horizontal axis by the angular separation between retrieved profiles) the retrieved ozone ESD [see Eq. (5)] averaged over all the retrieval-grid points along the full orbit (left) and the behavior of the χ_R^2 defined in Eq. (6) (right).

As expected,[5–7] the observed average ESD (Fig. 2, left) increases when the horizontal resolution is refined. However, around the value corresponding to the reference-retrieval setup, the ESD does not change as rapidly as expected on the basis of earlier studies on the vertical resolution of limb-sounders.[5] This indicates that the sensitivity of the selected MIPAS measurements to the horizontal variability of the atmosphere encountered along the line of sight is significant and offers the possibility of increasing the horizontal resolution by paying a relatively low cost in terms of retrieval precision. In particular, Fig. 2, left, suggests that the horizontal resolution of MIPAS measurements can be doubled with respect to the reference setup at the cost of an increment of a factor between 2 and 3 in the ESD.

The maps reported in the left column of Fig. 3 show as a function of altitude the geographical distribution of the ESD resulting from a few selected values of the horizontal resolution of the retrieval. In these maps on the horizontal scale is reported the orbital coordinate defined as a polar angle originating at the North Pole and spanning the orbit plane over its 360° extension. In Fig. 3 the overall degradation of the ESD obtained when the horizontal resolution is increased is evident; however, the extent of the degradation depends significantly on the altitude. To highlight this dependence, in Table 2 we report the average ESD as a function of altitude for four different values of the horizontal resolution. In Table 2 we show that the altitude region in which the trade-off between precision and horizontal resolution is most favorable coincides with the peak of the ozone distribution, where the sensitivity of the observations to the retrieval parameters is expected to be the maximum.[8]

To verify the overall consistency of our simulated retrievals, we also checked the behavior of the reduced chi-square [see Eq. (6)] as a function of the horizontal resolution. This behavior is reported in

Table 1. Horizontal Resolution of the Retrieval Grids Considered in the Trade-off Tests with Nominal MIPAS Observation Plan and Variable Retrieval Grid

Number of Retrieved Profiles per Orbit	Angular Spatial Separation between Profiles (deg)	Horizontal Linear Separation at Earth's Surface between Retrieved Profiles (kilometers)
25	14.4	1600
37	9.7	1078
40	9.0	1000
50	7.2	800
60	6.0	667
75	**4.8**	**533**
100	3.6	400
150	2.4	267
225	1.6	178
300	1.2	133

Note: The boldface entries refer to the so-called reference-retrieval setup in which one ozone profile is retrieved per measured limb-scan.

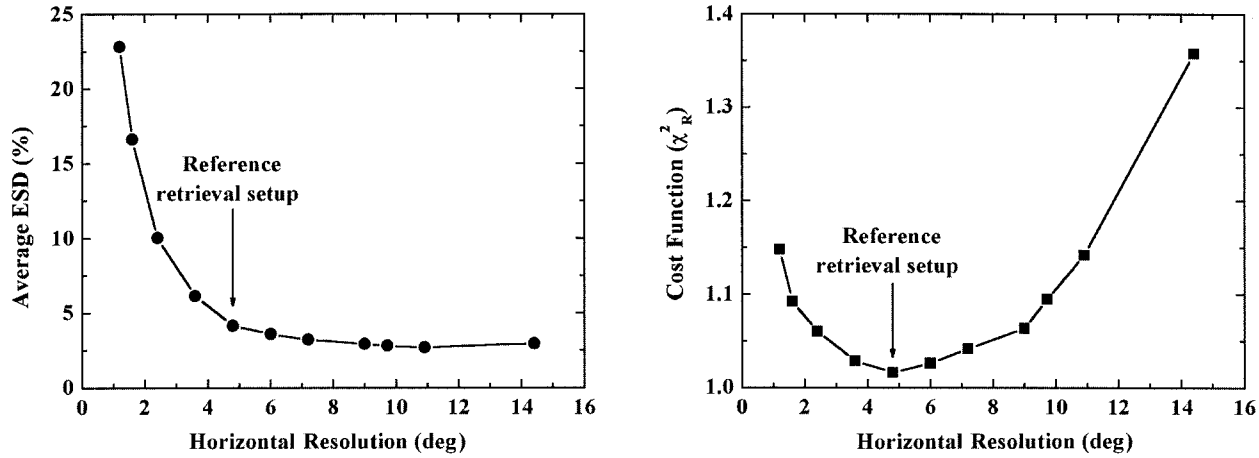

Fig. 2. Left, ESD of the retrieved ozone and, right, reduced chi-square as a function of the horizontal resolution quantified in terms of the angular separation between retrieved profiles. The plots represent the trade-off obtained with the variable retrieval grid and nominal measurement grid. Points marked with an arrow refer to the reference retrieval setup in which one vertical profile is retrieved per measured limb-scan.

Fig. 2, right. The χ_R^2 shows a minimum corresponding to the reference-retrieval setup. This minimum is due to the horizontal step of the retrieval grid in the reference setup roughly matching the horizontal resolution of the atmospheric model used to generate the synthetic observations. For retrieval grids coarser than in the reference setup χ_R^2 increases because in this case the forward model in the retrieval is no longer able to capture the horizontal variability of the atmosphere and therefore to fit the observations properly. For retrieval grids finer than in the reference setup the χ_R^2 increases as well because the redundancy of the retrieval grid is not useful in reducing the residuals of the fit while it significantly decreases the denominator of Eq. (6). (The horizontal variability of the atmosphere has already been resolved with the reference-retrieval grid.)

We also compared the deviation of the retrieved profiles from the true values with their ESDs. In general, for retrieval grids finer than or equal to the grid of the reference atmosphere the deviations are smaller than the ESD, thus proving the self-consistency of our forward and retrieval schemes. As an example of this self-consistency, in Fig. 4 we report the ratio between the absolute differences, retrieved-minus-true ozone profiles and the related ESD for the test retrieval performed with the horizontal resolution improved by a factor of 2 with respect to the nominal. From Fig. 4 we can see that, as expected from the statistics,[23] in the absence of a smoothing error the values of this ratio are generally below unity.

5. Trade-off Study Based on the Change in Spectral Resolution

In the second set of trade-off tests the improvement in horizontal resolution was obtained by degrading the spectral resolution. The MIPAS interferometer was designed to acquire interferograms with a constant speed of the interferometric mirror. This speed is determined by the sensitivity of the detectors and cannot be increased beyond the value used in the nominal measurement plan. With this constraint the possible strategies for increasing the number of measured limb-scans along the orbit consist of (a) limiting the altitude range of the acquired limb-scans, (b) decreasing the vertical sampling of the limb-scans, and (c) decreasing the spectral resolution (i.e., the maximum path difference of the measured interferograms). In all cases the time interval required for measuring a limb-scan turns out to be reduced with respect to the nominal measurement plan, in cases (a) and (b) because fewer sweeps per limb-scan are measured, in case (c) because the time interval necessary to measure the individual interferograms is reduced compared with the case of maximum spectral resolution.

Within the unconstrained least-squares approach, strategy (a) is not practical because the retrieval of profiles from limb-scans covering a limited altitude range was proved to be affected by large systematic errors due to the assumption of the profile shape above the uppermost and below the lowermost (due to the finite instrument FOV) retrieval altitudes.[24,25] Strategy (b) gains horizontal resolution at the cost of vertical resolution. Therefore in this study we considered only strategy (c). In Fig. 1(c) we show a scheme illustrating a measurement plan in which the spectral resolution of the instrument has deteriorated by a factor of 4, and consequently the number of measured limb-scans per orbit has increased with respect to the nominal plan. For simplicity we consider the number of measured scans per orbit as increasing inversely proportional to the spectral resolution. This means that, compared with the real instrument configuration, we ignore the dead-time interval required at the end of each limb-view measurement for reversing the interferometric mirror speed and for repositioning the limb-scanning mirror. This simplification was introduced to avoid a horizon-

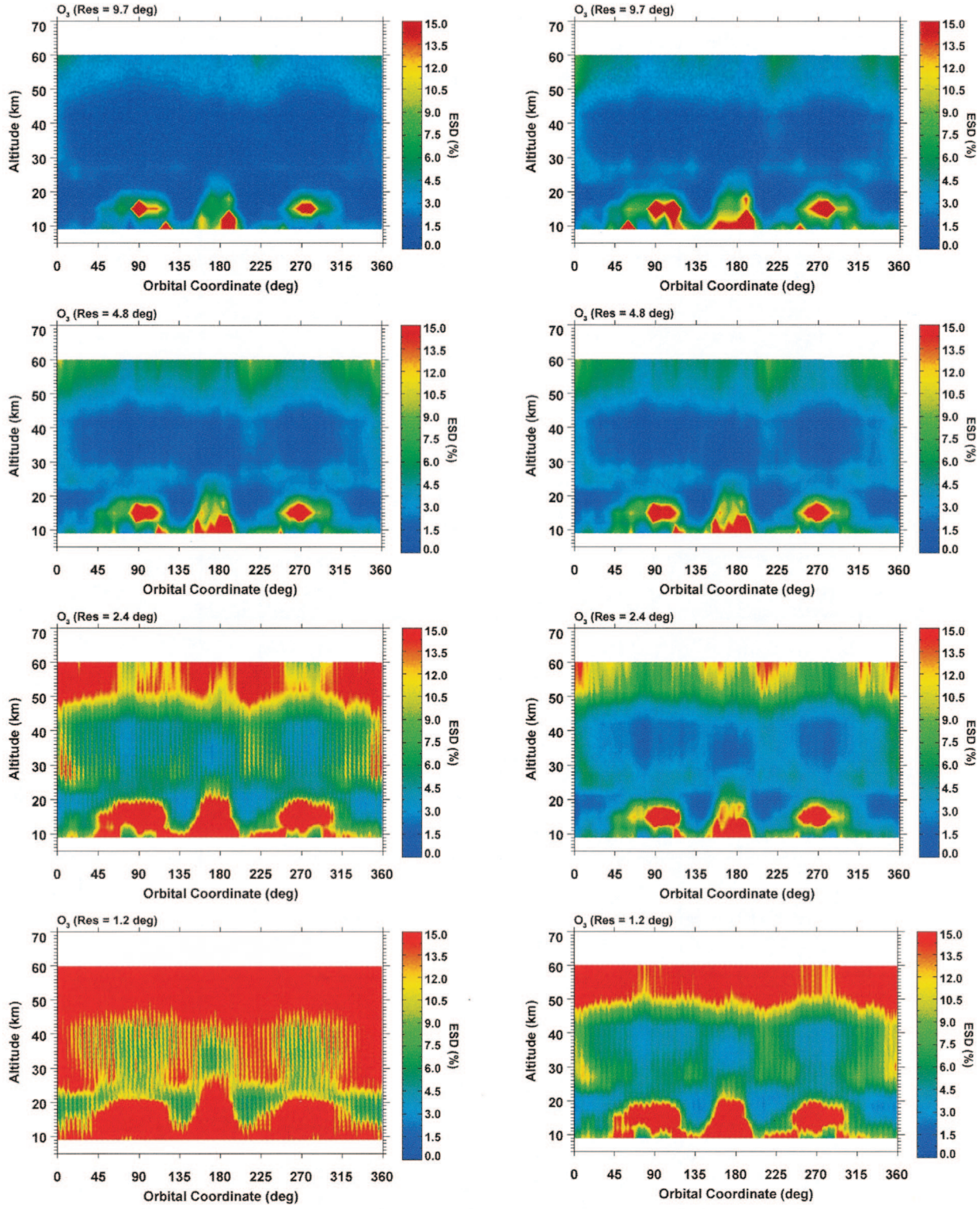

Fig. 3. Geographical distribution of the ESD for ozone retrievals: left, trade-off tests with nominal measurement mode and different horizontal resolutions attained by changing the retrieval grid; right, trade-off tests in which different horizontal resolutions are attained by changing the measurement grid. The horizontal resolution is indicated at the top of each map.

tal dephasing of measurement grids relating to different spectral resolutions. Such dephasing would make the comparison of the different retrieval setups considered in the study more difficult. The neglected dead time for MIPAS is much smaller than the time interval actually needed to acquire an interferogram, at least for spectral resolutions better or equal to one fourth of the nominal one. Therefore this approximation has no effect on the conclusions of this study.

Table 2. Estimated Standard Deviation Averaged along the Full Orbit for the Retrieval Altitudes

Altitude (km)	Average ESD (%)			
	A	B	C	D
60	4.1	6.6	14.8	37.5
52	3.0	4.8	14.8	35.3
47	2.3	3.4	9.6	22.1
42	1.4	2.1	5.7	13.2
39	1.5	2.1	5.9	13.3
36	1.4	2.0	5.8	12.5
33	1.5	2.0	6.0	12.7
30	1.6	2.3	6.8	14.0
27	2.0	3.0	7.0	13.9
24	1.9	3.1	5.9	11.5
21	1.8	2.6	5.2	10.2
18	3.1	4.4	9.9	20.6
15	6.3	10.0	21.7	42.3
12	4.5	6.0	13.4	30.0
9	5.7	8.2	17.8	53.6

Note: Columns A, B, C, and D refer to horizontal resolutions of 1078, 533 (reference case), 267, and 133 km, respectively. This table refers to the tests reported in Section 4.

Since the retrieval algorithm makes use of only a few narrow spectral intervals for the inversion procedure, particular care must be used in interpreting the results obtained with a spectral resolution different from the nominal one. Actually in a given microwindow the spectral features sensitive to the target gas of the retrieval are expected to spread outside the boundaries of the microwindow itself when the spectral resolution is reduced. Since the objective of our study was limited to studying the trade-off between precision and horizontal resolution, we did not want to be biased by these side effects. For this reason the test retrievals shown in this section were performed with microwindows obtained by extending the boundaries of the nominal set of microwindows optimized for the maximum MIPAS resolution. The frequency extension was obtained by changing the spectral sampling step, as explained in Subsection 3.A, and by conserving the total number of independent spectral grid points per analyzed microwindow.

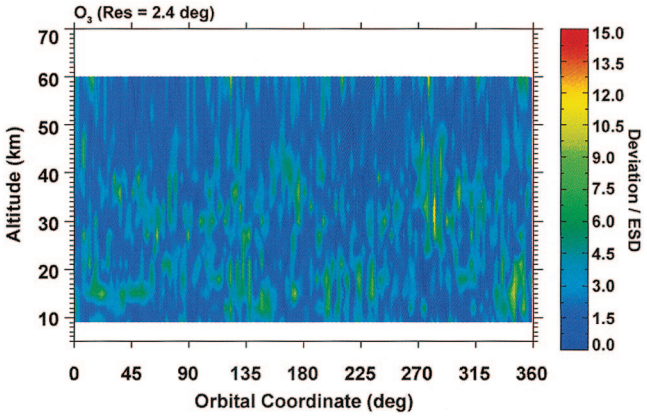

Fig. 4. Ozone retrieval. The map shows the absolute ratio between the deviations (retrieved − true profiles) and the ESD. The map refers to a test case with the nominal measurement grid and the horizontal resolution doubled with respect to the reference case.

With this strategy all the information contained in the original interval is retained in the retrievals. Actually the comparability of the results also requires that the process of extending the microwindows should not lead to a net increment of the retrieval sensitivity to the target parameters due to the possible inclusion in the extended microwindow of the spectral lines of the retrieved species lying outside the original microwindow. According to these considerations, the spectral lines of the target species lying outside the original microwindows were masked by labeling them as belonging to a virtual gas having the same VMR distribution of the target gas. With this trick the overall opacity of the considered spectral region is not modified, and the masked lines do not alter the sensitivity of the retrieval to the target parameters since they do not contribute to the Jacobian $\mathbf{K}$ in Eq. (2). The performance of these test retrievals is then interpreted only in terms of the changes introduced in the measurement and in the retrieval grids. In this set of tests the retrieval grid has been set to one profile per measured limb-scan.

As for the results reported in Section 4, in Fig. 5 we show the average values of the ESD (left) and of χ_R^2 (right) as a function of the horizontal resolution. The points marked with an arrow in Fig. 5 refer to the reference-retrieval setup with nominal spectral resolution. For comparability with Fig. 2, in Fig. 5 we also report the result of a test corresponding to the unrealistic plan of spectral resolution enhanced by a factor of 2 with respect to the nominal value.

The considerations for Fig. 2 apply to the plots in Fig. 5 too; however, in this case both the ESD and the χ_R^2 do not increase as rapidly with the increasing horizontal resolution as in Fig. 2 (note the different vertical scales in Figs. 2 and 5). Therefore the strategy of varying the spectral resolution leads to a more favorable trade-off than in the case of the constant measurement grid. Figure 3 (right) shows the geographical distribution of the ESD obtained from the test retrievals performed in this part of the study. A comparison of the maps in the right column with the maps in the left column in Fig. 3 confirms that in general the trade-off between precision and horizontal resolution is more favorable when the spectral resolution is degraded in order to get a finer horizontal sampling of the atmosphere. The altitude dependence of the trade-off obtained within the strategy considered in this section is very similar to that obtained in the case of the variable retrieval grid. Therefore we are not showing a table similar to Table 2 for the approach with a variable spectral resolution.

In the case of real observations the strategy reported in this section should be implemented with care. In particular, whenever the spectral resolution is degraded with respect to the nominal measurement plan, the effect of nontarget species contributing to the radiance in the spectral intervals

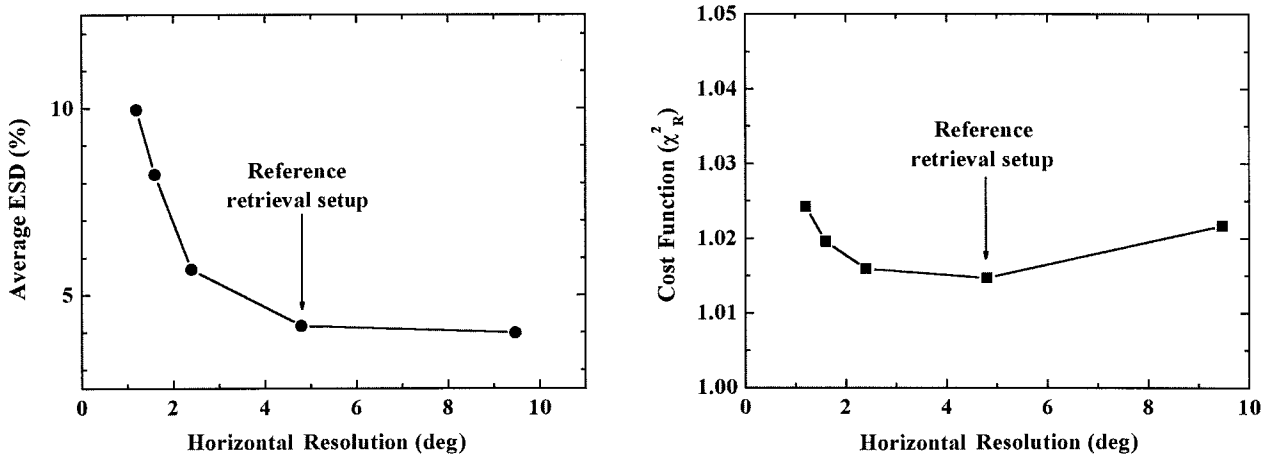

Fig. 5. Left, ESD of the retrieved ozone, and, right, reduced chi-square as a function of the horizontal resolution quantified in terms of the angular separation between the retrieved profiles. The plots represent the trade-off obtained by varying the spectral resolution. The points marked with an arrow refer to the reference-retrieval setup.

used for the retrieval is expected to increase. Therefore the retrieval error component due to imperfect knowledge of the atmospheric distribution of these interfering nontarget species (not evaluated in this study) may become important. However, the enhancement of this error component is not expected to invalidate the results of this trade-off study. In fact, given the wide amplitude of the spectral bands measured by MIPAS, the retrieval accuracy can be recovered including additional spectral intervals in the data set of the analyzed observations and/or using multitarget retrieval techniques.[26]

6. Discussion and Conclusions

In this paper we report the results of a study aimed at assessing the trade-offs between the horizontal resolution and the precision of the ozone VMR profiles that can be retrieved from MIPAS–ENVISAT measurements. The capabilities of the geo-fit[10] two-dimensional retrieval algorithm have been exploited to test different retrieval and observation plans. A general outcome of this study is that the horizontal resolution of the retrieved profiles can be improved with respect to the nominal value (~530 km at the Earth's surface) that is determined by the separation between the measured limb-scans. Two different strategies have been considered for changing the horizontal resolution of the retrieval products:

(1) Nominal MIPAS measurements are analyzed on a horizontal retrieval grid that is different from the measurement grid. In this case improvement of a factor of 2 in the horizontal resolution (from 530 to 265 km) leads to a factor of between 2 and 3 of degradation for the ESD of the retrieved ozone profiles. (On average the ESD increases from the value of 4% to 10%.)

(2) A finer horizontal sampling of the atmosphere can be obtained by operating the MIPAS instrument with a spectral resolution degraded with respect to its maximum value used in the nominal measurement plan. Halving the spectral resolution allows measuring a limb-scan approximately every 265 km. In these conditions, retrieving one ozone profile per measured limb-scan leads to a 40% increase of the average ESD with respect to the standard plan. An increase of a factor of 2 in the ESD corresponds to observation conditions that provide ~180 km of horizontal resolution.

A comparison of the two strategies indicates that the most suitable strategy for improving the horizontal resolution of the atmospheric profiles is to degrade the spectral resolution. However, to test this strategy, assumptions had to be made that do not take into account the effect of error components due to interfering, nontarget species, and we expect that the favorable behavior of the trade-off could worsen when these errors are taken into account. Current knowledge of these error components enables us, however, to state that a proper error budget is not going to invalidate the overall results obtained with the second strategy.

Note that, if a given objective for the accuracy of the retrieved profiles has to be met, given the wide amplitude of the spectral bands measured by MIPAS, the accuracy of the retrieved products can be improved by including additional spectral intervals in the data set of the analyzed observations and/or by using joint retrieval techniques.[26]

The results of this study refer to the MIPAS–ENVISAT experiment. However, the rationale of the adopted strategies is applicable to any limb-scanning satellite experiment measuring along the orbit track. The specific trade-off is expected to depend on the features of the considered experiment.

This study was supported by the European Space Agency (ESA) through ESRIN (European Space Research Institute) contract 16700/02/I-LG.

References

1. M. Ridolfi, B. Carli, M. Carlotti, T. von Clarmann, B. M. Dinelli, A. Dudhia, J.-M. Flaud, M. Höpfner, P. E. Morris, P. Raspollini, G. Stiller, and R. J. Wells, "Optimized forward model and retrieval scheme for MIPAS near-real-time data processing," Appl. Opt. **39,** 1323–1340 (2000).
2. M. Carlotti, "Global fit approach to the analysis of limb-scanning atmospheric measurements," Appl. Opt. **27,** 3250–3254 (1988).
3. G. E. Backus and F. Gilbert, "Uniqueness in the inversion of inaccurate gross Earth data," Philos. Trans. R. Soc. London Ser. A **266,** 123–192 (1970).
4. B. J. Conrath, "Vertical resolution of temperature profiles obtained from remote radiation measurements," J. Atmos. Sci. **29,** 1262–1271 (1972).
5. M. Carlotti and B. Carli, "Approach to the design and data analysis of a limb-scanning experiment," Appl. Opt. **33,** 3237–3249 (1994).
6. M. Carlotti and M. Ridolfi, "Derivation of temperature and pressure from submillimetric limb observations," Appl. Opt. **38,** 2398–2409 (1999).
7. H. K. Roscoe and J. G. T. Hill, "Vertical resolution of oversampled limb-sounding measurements from satellites and aircraft," J. Quant. Spectrosc. Radiat. Transfer **72,** 237–248 (2002).
8. B. Carli, M. Ridolfi, P. Raspollini, B. M. Dinelli, A. Dudhia, and G. Echle, "Study of the retrieval of atmospheric trace gas profiles from infrared spectra," Final Report, ESA study 12055-96-NL-CN (European Space Agency, Noordwijk, The Netherlands, 1998).
9. A. N. Tikhonov and V. Y. Arsenin, *Solutions of Ill-Posed Problems* (V. H. Winston, Washington, D.C., 1977).
10. M. Carlotti, B. M. Dinelli, P. Raspollini, and M. Ridolfi, "Geo-fit approach to the analysis of satellite limb-scanning measurements," Appl. Opt. **40,** 1872–1885 (2001).
11. A. Dudhia, Department of Atmospheric, Oceanic, and Planetary Physics, Oxford University, Clarendon Laboratory, Parks Road, Oxford, OX1 3PU, UK (personal communication, 2004).
12. C. D. Rodgers, *Inverse Methods for Atmospheric Sounding: Theory and Practice*, Series on Atmospheric, Oceanic, and Planetary Physics, Vol. 2 (World Scientific, Singapore, 2000).
13. T. von Clarmann and G. Echle, "Selection of optimized microwindows for atmospheric spectroscopy," Appl. Opt. **37,** 7661–7669 (1998).
14. M. P. Chipperfield, "Multiannual simulations with a three-dimensional chemical transport model," J. Geophys. Res. **104,** 1781–1805 (1999).
15. S. A. Clough, F. X. Kneizys, and R. W. Davis, "Line shape and the water vapor continuum," Atmos. Res. **23,** 229–241 (1989).
16. T. von Clarmann, M. Höpfner, B. Funke, M. López-Puertas, A. Dudhia, V. Jay, F. Schreier, M. Ridolfi, S. Ceccherini, B. J. Kerridge, J. Reburn, and R. Siddans, "Modeling of atmospheric mid-infrared radiative transfer: the AMIL2DA algorithm intercomparison experiment," J. Quant. Spectrosc. Radiat. Transfer **78,** 381–407 (2003).
17. M. Ridolfi, D. Alpaslan, B. Carli, M. Carlotti, E. Castelli, S. Ceccherini, B. M. Dinelli, A. Dudhia, J.-M. Flaud, M. Höpfner, V. Jay, L. Magnani, H. Oelhaf, V. Payne, C. Piccolo, M. Prosperi, P. Raspollini, J. Remedios, and R. Spang, "MIPAS level 2 processor performance and verification," in *Proceedings, ENVISAT Validation Workshop of European Space Research Institute, 9–13 November 2002, The Netherlands*, ESA SP-531, Noordwijk, The Netherlands (European Space Agency, Noordwijk, The Netherlands, 2002).
18. M. Endemann, "MIPAS instrument concept and performance," in *Proceedings of the European Symposium on Atmospheric Measurements from Space*, ISSN 1022-6656 (European Space Research and Technology Center–European Space Agency, Noordwijk, The Netherlands, 1999), WPP-161, Vol. 1, pp. 29–43.
19. B. Carli, M. Carlotti, M. Höpfner, P. Raspollini, and M. Ridolfi, "MIPAS level 2 algorithm theoretical baseline document," Tech. Rep. ESA contract 11717/95/NL/CN (European Space Agency, Noordwijk, The Netherlands, 2001).
20. R. H. Norton and R. Beer, "New apodizing functions for Fourier spectrometry," J. Opt. Soc. Am. **66,** 259–264 (1976); errata J. Opt. Soc. Am. **67,** 419 (1977).
21. M. Ridolfi, "Development of algorithms for the exploitation of MIPAS special modes measurements," European Space Agency–European Space Research Institute contract 16700/02/I-LG (2003), http://www.fci.unibo.it/~ridolfi/mipas_sm_rationale.html.
22. G. Redaelli, Dipartimento di Fisica, Università degli Studi dell'Aquila, Via Vetoio, Coppito, 67010 L'Aquila, Italy (personal communication, 2004).
23. P. R. Bevington and D. K. Robinson, *Data Reduction and Error Analysis for the Physical Sciences*, 3rd ed. (McGraw-Hill, New York, 2003).
24. P. Raspollini, D. Alpaslan, B. Carli, M. Carlotti, E. Castelli, S. Ceccherini, B. M. Dinelli, A. Dudhia, J.-M. Flaud, M. Hoepfner, V. Jay, L. Magnani, H. Oelhaf, C. Piccolo, M. Prosperi, J. Remedios, M. Ridolfi, and R. Spang, "Level 2 near-real-time analysis of MIPAS measurements on ENVISAT: updated performance assessment," European Geophysical Society –American Geophysical Union–European Union of Geosciences joint assembly, Nice, 6–11 April 2003.
25. A. Dudhia, "MIPAS microwindow error analysis," (2002), http://www.atm.ox.ac.uk/group/mipas/err/.
26. B. M. Dinelli, D. Alpaslan, M. Carlotti, L. Magnani, and M. Ridolfi, "Multitarget retrieval (MTR): the simultaneous retrieval of pressure, temperature and volume mixing ratio profiles from limb-scanning atmospheric measurements," J. Quant. Spectrosc. Radiat. Transfer **84,** 141–157 (2004).